A pseudopotential method for investigating the surface roughness effect in ultrathin body transistors

2008 J. Phys.: Condens. Matter 20 235229

(http://iopscience.iop.org/0953-8984/20/23/235229)

J. Phys.: Condens. Matter **20** (2008) 235229 (5pp) doi:10.1088/0953-8984/20/23/235229

A pseudopotential method for investigating the surface roughness effect in ultrathin body transistors

Zhen-Gang Zhu, Gengchiau Liang, Ming-Fu Li and Ganesh Samudra

Silicon Nano-Device Laboratory (SNDL), ECE Department, National University of Singapore, Singapore

Received 22 January 2008, in final form 1 April 2008
Published 9 May 2008
Online at stacks.iop.org/JPhysCM/20/235229

Abstract

An atomistic method based on the diffraction pseudopotential model is established, for investigating the surface roughness (SR) effect in ultrathin body double-gate metal–oxide–semiconductor field effect transistors. The scattering of electrons due to atoms and vacancies responsible for roughness results from a three-dimensional effective field, and its planar components provide essentially roughness scattering, while a vertical effective field is the source of scattering in the method developed in which roughness is treated as a semiclassical barrier fluctuation. The present model involves a stronger effect on mobility than the previously developed one and results in an excellent fit, as regards mobility, to the reported experimental data. The extracted SR parameter also matches the observed value.

(Some figures in this article are in colour only in the electronic version)

Ultrathin body (UTB) metal–oxide–semiconductor field effect transistors (MOSFET) have been considered important for controlling short channel effects [1]. And surface roughness (SR) at the Si–SiO_2 interface in the MOSFET is considered to be inherent to the space charge layer and to be one of the dominant scattering mechanisms, especially at high electron concentrations, in present-day MOSFET [2, 3]. Furthermore, it was demonstrated that an atomic level thickness fluctuation has a significant impact on the threshold voltage, gate channel capacitance, and carrier mobility in a UTB MOSFET when the body thickness is below 4 nm [4].

It is generally believed that the exact properties of the SR have not been established very well [5]. The early semiclassical model of the SR [6–8] was based on the assumption that continuous fluctuation of the barrier potential provides the SR scattering mechanism, and it was extended to investigate the role of the SR in transport in UTB MOSFET recently [9, 10]. However the SR parameter extracted from this model does not match the experimental finding very well [4, 10] (see details in the text). In this case, it is reasonable to believe that the approximation of the continuous barrier model is no longer adequate when MOSFET structures have entered into the nanoscale regime. And it is necessary to establish a new and more accurate microscopic model of the SR which goes beyond the semiclassical one. In this paper, we use a pseudopotential (PS) to describe the interaction of the SR scattering centers (SRSCs) and establish a largely analytical model at a microscopic level. Although an attempt to treat the SR at the atomic level was made on the basis of *ab initio* calculation [11], it is still important and valuable to explore this more deeply. Furthermore, our model provides definite SR parameters which can be examined in experiments. It is shown that the mobility derived and the SR parameter extracted from the present model fit the experimental data very well, which is much better than the semiclassical model outcome. It should be noted that the present model is essentially different to the latter, because the effective electric field (EEF) of SRSCs in the latter is a local, planar-coordinate-dependent vertical field, while it is a 3D, nonlocal EEF in our model.

Figure 1(a) shows a schematic diagram for Si(100) film. The crystal structure is described in terms of a 2D lattice attached with basis atoms [12], where the 2D lattice is defined on the top surface (TS), and 2D Wigner–Seitz (WS) cells (figure 1(b)) are given by $\vec{\rho}_i = (a_0/2)(i_x \mathbf{e}_x + i_y \mathbf{e}_y)$, where $a_0 = 5.4307$ Å is the crystal constant, $i_{x\,(y)}$ are integers. The zero point in the z direction is set at the bottom surface (BS) while $z = L$ for the TS. All the atoms between the BS and the TS form a perfect film (PF). Additional atoms (aa) and

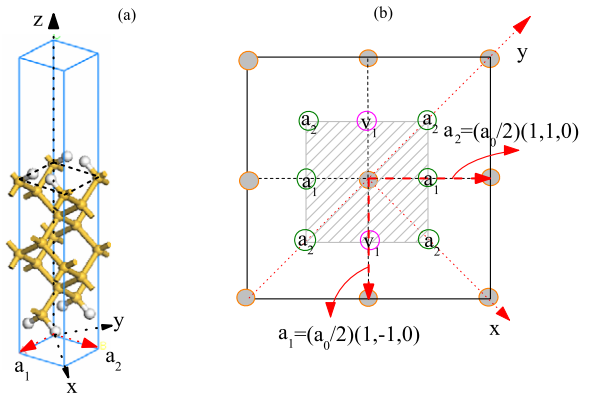

Figure 1. A schematic Si(100) thin film and 2D Wigner–Seitz cell for the top surface are shown in (a) and (b) respectively. Shaded circles in (b) are Si atoms, $a_{1\,(2)}$ and $v_{1\,(2)}$ are positions available for the first (second) aa and the first (second) va. v_2 is below a_2.

vacancies (va) introduce SRSCs and the sites available for them symmetrically around the central atom of the WS cell (figure 1(b)).

It is assumed that SR only occurs around the TS. It will be straightforward to extend it to the BS. The single-particle Hamiltonian is given in terms of the diffraction PS model [13] as

$$H = T + \sum_{i\vec{\xi}_i} U^{\mathrm{PS}}(\mathbf{r} - \vec{\rho}_i - \vec{\xi}_i) + \sum_{j\vec{\xi}_{j\mathrm{SR}}} U^{\mathrm{PS}}(\mathbf{r} - \vec{\rho}_j - L\mathbf{e}_z - \vec{\xi}_{j\mathrm{SR}}) + V_B(\vec{\rho}, z), \quad (1)$$

where the first term is the kinetic energy, the second term is the potential for all atoms in the PF except the atoms on the TS, and $\vec{\xi}_i$ are the coordinates of basis atoms (relative to the lattice point) whose x and y components are on the ith 2D WS. The third term in (1) accounts for the potentials of SRSCs, i, j run over all WSs, $\vec{\xi}_{j\mathrm{SR}}$ are relative coordinates of SRSCs referenced to $\mathbf{r}_j = \vec{\rho}_j + L\mathbf{e}_z$ (when $\vec{\xi}_{j\mathrm{SR}} = 0$, this term gives the potential of atoms on the TS; otherwise it gives the potentials of the aa or the va). Furthermore, the fourth term in (1) is from the barrier potential in which the barrier SR is described by means of the fluctuation of the barrier boundaries [8]. It can be expanded around the TS, the zero-order V_0 is for the PF and the first-order V_1 accounts for the barrier roughness (BR) [8].

Expanding the third term around the TS, i.e. $\vec{\rho} - \vec{\rho}_j$ and $z - L$, we get

$$U^{\mathrm{PS}}(\mathbf{r}-\mathbf{r}_j-\vec{\xi}_{j\mathrm{SR}}) = U^{\mathrm{PS}}(\mathbf{r}-\mathbf{r}_j) - [\nabla U^{\mathrm{PS}}(\mathbf{r}-\mathbf{r}_j)]\cdot\vec{\xi}_{j\mathrm{SR}}, \quad (2)$$

where $\vec{\xi}_{j\mathrm{SR}} = \vec{\xi}_{j\mathrm{SR}\parallel} + \vec{\xi}_{j\mathrm{SR}z}$, $\vec{\xi}_{j\mathrm{SR}\parallel}$ and $\vec{\xi}_{j\mathrm{SR}z}$ are components in xy plane and z direction. The summation over j in the first term in equation (2) gives the PS of the atoms on the TS, which is combined with the second term in equation (1) to give the total PS of the PF, i.e. $V_{\mathrm{PF}}^{\mathrm{PS}} = \sum_{i\vec{\xi}_i} U^{\mathrm{PS}}(\mathbf{r} - \vec{\rho}_i - \vec{\xi}_i)$, including all atoms in the PF. The second term in equation (2) is the effective field caused by SRSCs (briefly: atomic roughness (AR)).

According to the diffraction model [13], we regard $H_0 = T + V_0$ as the unperturbed system which describes the free electrons in a quantum well with perfect boundaries. Its eigenfunctions can be written as

$$\phi_{n\mathbf{k}}(\mathbf{r}) = \frac{1}{2\mathrm{i}}\sqrt{\frac{2}{SL}}(\exp(\mathrm{i}\mathbf{K}_{n+}\cdot\mathbf{r}) - \exp(\mathrm{i}\mathbf{K}_{n-}\cdot\mathbf{r})), \quad (3)$$

where $S = NS_0$ is the area of the UTB surface, N is the total number of 2D WSs, $S_0 = a_0^2/2$, $\mathbf{K}_{n\pm} = \mathbf{k} \pm k_{nz}\mathbf{e}_z$ is a 3D vector in the reciprocal space, $\mathbf{k}$ is a 2D wavevector, $k_{nz} = n\pi/L$, $n = 1, 2, \ldots$, and $\mathbf{r}$ is a 3D vector in real space. The Hamiltonian for the PF is $H_{\mathrm{PF}} = H_0 + V_{\mathrm{PF}}^{\mathrm{PS}}$. Thus the perturbation Hamiltonian of the SR will be $H_{\mathrm{pert}}^{\mathrm{SR}} = H - H_{\mathrm{PF}}$. The strategy of calculation of the matrix elements (ME) of the SR is calculating the ME of H and H_{PF} by using the diffraction model.

We first calculate the transition probability for H_{PF} arising from the potential $V_{\mathrm{PF}}^{\mathrm{PS}}$ [13]. A structure factor $\sum_i \mathrm{e}^{\mathrm{i}\Delta\mathbf{k}\cdot\vec{\rho}_i}$ is present in the ME, which is zero if $\Delta\mathbf{k}$ is not on a 2D lattice formed by reciprocal primitive vectors. Otherwise, it equals 1. However, $\Delta\mathbf{k}$ being on a 2D lattice is just equivalent to the Bragg diffraction condition, which gives rise to the standing waves in the crystal and does not contribute to any scattering which may cause resistance to the motion of electrons. This result also manifests itself in the ME of H in which $V_{\mathrm{PF}}^{\mathrm{PS}}$ is present as well. Therefore, the scattering rates caused by SR are contributed from two sources: one is from the AR, the other is from the effect of the BR (see above). The latter is considered as the only source of SR in the method developed previously [2, 3, 8, 9]. The former term gives an atomistic view and a new scattering mechanism for SR which we shall investigate in detail. Combination of the two sources gives the effect of $H_{\mathrm{pert}}^{\mathrm{SR}}$, and we use $V_{\mathrm{SR}}^{\mathrm{PS}}$ to express the AR's contribution (see equations (4), (5) and (6)).

Transition matrix. The transition matrix caused by AR in terms of equation (3) is

$$\langle n'\mathbf{k}'|V_{\mathrm{SR}}^{\mathrm{PS}}|n\mathbf{k}\rangle = -f_V \sum_{j\vec{\xi}_j g} \delta_g \vec{\xi}_j \cdot \mathbf{E}_{\mathrm{avg}}(\mathbf{Q}_g)\mathrm{e}^{-\mathrm{i}\mathbf{Q}_g\cdot\mathbf{r}_j}, \quad (4)$$

where $f_V = \frac{f_0}{N}$, $f_0 = \frac{\Omega_{\mathrm{atom}}}{2S_0L}$, Ω_{atom} is the atomic volume of Si atoms, $g = 1, 2, 3$, and 4, $\delta_{1\,(4)} = 1$, $\delta_{2\,(3)} = -1$, $\mathbf{Q}_{1\,(2)} = \mathbf{K}'_{n'+} - \mathbf{K}_{n+(n-)}$, $\mathbf{Q}_{3\,(4)} = \mathbf{K}'_{n'-} - \mathbf{K}_{n+(n-)}$, and $\mathbf{E}_{\mathrm{avg}}(\mathbf{Q}) = (1/\Omega_{\mathrm{atom}})\int \exp(-\mathrm{i}\mathbf{Q}\cdot\mathbf{r})\nabla U^{\mathrm{PS}}(\mathbf{r})\mathrm{d}\mathbf{r}$ is an effective field. Choosing one term in the summation in equation (4), i.e. $g = 1$ and $\xi_{jz}E_{\mathrm{avg},z}$, its ME is $\langle|V^{\mathrm{PS}}|\rangle_{g=1,z} = -f_V E_{\mathrm{avg},z}(\mathbf{Q}_1)\exp(-\mathrm{i}Q_{1z}L)\sum_{i_x,i_y}\exp(-\mathrm{i}(Q_{1x}\rho_{ix} + Q_{1y}\rho_{iy}))\bar{\xi}_z(i_x, i_y)$, where i_x, i_y cover all WSs, and $\bar{\xi}_z(i_x, i_y) = \sum_{\xi_{iz}} \xi_z(i_x, i_y)$ is a random number and the total variation of all SRSCs on the (i_x, i_y)th WS. For WSs with aa (va) on it, $\bar{\xi}_z > 0$ (<0). $\langle\bar{\xi}_z\rangle = 0$ can be obtained. $I_{x\,(y)}$ is the total number of summation variables $i_{x\,(y)}$ and $N = I_xI_y$; we have $\bar{\xi}_z(Q_{1x}, Q_{1y}) = (1/N)\sum_{i_x,i_y\in\text{all WSs}}\bar{\xi}_z(i_x, i_y)\exp(-\mathrm{i}(Q_{1x}\rho_{ix} + Q_{1y}\rho_{iy}))$ is the Fourier transformation of $\bar{\xi}_z(i_x, i_y)$ defined on discrete primitive vectors [5, 12].

For other components, we still have $\langle\bar{\xi}_x\rangle = \langle\bar{\xi}_y\rangle = 0$. The same calculation can also be applied to these two. Thus the transition matrix is

$$\langle n'\mathbf{k}'|V_{\mathrm{SR}}^{\mathrm{PS}}|n\mathbf{k}\rangle = -f_0 \sum_g \delta_g \vec{\bar{E}}(\mathbf{Q}_g)\cdot\vec{\bar{\xi}}(Q_{gx}, Q_{gy}) \quad (5)$$

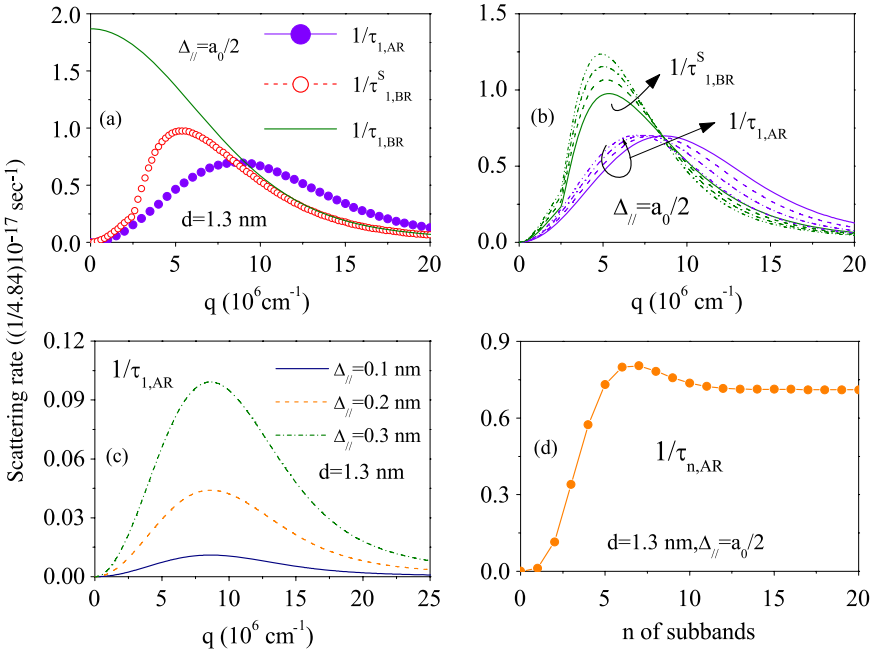

Figure 2. The variations of the scattering rate are shown with q in (a), with q for different d in (b), with q for different $\Delta_{\parallel}$ in (c), and with number of subbands n in (d). The effective masses of Si are $m_t = 0.19m_0$, $m_l = 0.92m_0$, where m_0 is the bare mass of electrons, and the inversion charge density is set at $N_S = 1 \times 10^{12}$ cm^{-2}. The other parameters are as follows. (a) $L = a_0$. (b) $d = 1.3$, 1.4, 1.5 and 1.6 nm correspond to the solid, dashed, dash–dotted, and dash–dot–dotted lines, for $1/\tau_{1,\mathrm{AR}}$ and $1/\tau^S_{1,\mathrm{BR}}$. $L = a_0$. (c) $L = 1.5a_0$. (d) $L = 2a_0$, $q = 5 \times 10^6$ cm^{-1}.

where $\vec{\bar{E}}(\mathbf{Q}_g) = \mathrm{e}^{-\mathrm{i}Q_{gz}L}\mathbf{E}_{\mathrm{avg}}(\mathbf{Q}_g)$. Equation (5) accounts for the AR contribution. We assume that the coupling between AR and BR is weak; therefore the transition probability will be

$$|\langle n'\mathbf{k}'|H^{\mathrm{PS}}_{\mathrm{pert}}|n\mathbf{k}\rangle|^2 = |\langle n'\mathbf{k}'|V^{\mathrm{PS}}_{\mathrm{SR}}|n\mathbf{k}\rangle|^2 + |\langle|V_1|\rangle|^2, \qquad (6)$$

where $\langle|V_1|\rangle$ is the transition matrix of V_1 for the BR case.

Relaxation time and mobility. We can derive the relaxation time and mobility in 2D under the influence of SR by extending the 3D treatment of [14]. We shall consider the stationary and homogeneous system under the elastic ($k = k'$) and relaxation time approximations.

When the intersubband scattering is negligible, the relaxation time can be derived [3] as

$$\frac{1}{\tau_n} = \frac{2\pi}{\hbar}\sum_{\mathbf{k}'}|\langle n\mathbf{k}'|H^{\mathrm{PS}}_{\mathrm{pert}}|n\mathbf{k}\rangle|^2(1-\cos\theta)\delta(E(\mathbf{k}')-E(\mathbf{k})), \qquad (7)$$

where $E = E_n + E(\mathbf{k})$ is the total energy for an electron in a subband n with a 2D wavevector $\mathbf{k}$, and the individual ME are from equation (6).

The autocovariance function (ACVF) [5] is defined to characterize the SR behavior as $C_{x\,(y,z)}(i'_x, i'_y) = \langle\bar{\xi}_{x\,(y,z)}(i_x, i_y)\bar{\xi}_{x\,(y,z)}(i_x - i'_x, i_y - i'_y)\rangle$ and the power spectrum $\zeta(Q_x, Q_y)$ of this ACVF is just its Fourier transformation according to the Wiener–Kitchine theorem. It should be pointed out that the power spectrum in our model is actually a 3D function, which is different from the conventional 1D function in the BR case [3]. The power spectrum is usually assumed to be of the Gaussian [8, 15], exponential [16], or intermediate type [9, 17]. Because the averaged relative coordinates $\bar{\xi}_{x\,(y,z)}$ are all zero, we may regard the three components as independent of each other. Thus, we have

$$|\langle n'\mathbf{k}'|V^{\mathrm{PS}}_{\mathrm{SR}}|n\mathbf{k}\rangle|^2 = f_0^2\sum_{gg'}\delta_g\delta_{g'}[q_x^2\zeta_x + (Q_{gz}Q_{g'z})\zeta_z + q_y^2\zeta_y] \times [U^{\mathrm{PS}}(\mathbf{Q}_g)U^{\mathrm{PS}}(\mathbf{Q}_{g'})]\mathrm{e}^{\mathrm{i}L\Delta Q}, \qquad (8)$$

where $\zeta_{x\,(y,z)}$ all depend on q_x and q_y, $U^{\mathrm{PS}}(\mathbf{Q})$ is the atomic PS in reciprocal space, $\Delta Q = Q_{gz} - Q_{g'z}$. In (8), the second term is calculated to be zero.

In numerical calculation, a model PS for Si [18] is used. The power spectrum is assumed to be $\zeta_x(Q_x, Q_y) = \zeta_y(Q_x, Q_y) = \pi\Delta_{\parallel}^2 d^2\exp(-(Q_x^2+Q_y^2)d^2/4)$, where $\Delta_{\parallel}$ is the rms value of the roughness function, d is the autocovariance length. The potential of the barrier changes abruptly and discontinuously at the boundaries, which leads to a delta function there. Thus a zero expectation for the transition probability is derived for the BR term in our model. The roughness effect is in fact included by the AR term here. So in the following and all graphs, we refer AR to our model and BR to the previously developed methods [3, 8, 15]. The formulas for the scattering rate (SCR), transition matrix and mobility in the BR case are similar to those in [15]; the isotropic effective mass (EM) of GaAs is replaced by the longitudinal (transverse) EMs of Si, $\epsilon(q)$ is the screening dielectric function from [8], where $q = |\mathbf{k}'-\mathbf{k}|$. We use $1/\tau_{n,BR}$ to express the SCR without screening.

In figure 2(a), we compare the SCR for AR and BR cases with and without screening. Without screening, $1/\tau_{1,\mathrm{BR}}$ decreases monotonically with increasing q, and it has a finite value at $q = 0$ (long wavelength limit (LWL)). When the

screening is included, the SCR $1/\tau^{S}_{1,\mathrm{BR}}$ is dramatically changed at the LWL; it tends to zero when $q \to 0$ [19]. In this limit, the scattering from the barrier fluctuation is screened more profoundly. $1/\tau_{1,\mathrm{AR}}$ shows the same tendency at the LWL and it also tends to zero when q approaches larger values (short wavelength limit (SWL)). In the SWL, the AR case and BR case tend to be the same. Thus there are electrons with some moderate wavevectors that are efficiently scattered under the influence of SR for a given SR distribution.

The screening is crucial to the BR model. The first introduction of the screening effect in the conventional SR model is in [7]. However we note that the screening dielectric function was introduced into the expression without rigorous derivation [7, 8], simply by using the screening dielectric function which was derived for a Coulomb field caused by the charged impurities in the barrier (outside of the electron gas) [20]. The Coulomb potential of the charged impurity is a long range potential, while the barrier fluctuation induces a local EEF which only exists in a thin sheet of the fluctuation region whose thickness is determined by $\Delta_{\|}$ which is usually several Å [8, 17, 19]. This is comparable to the estimation of a typical screening length in Si of about 5.5 Å in [20]. Strictly speaking, it is necessary to give a detailed microscopic derivation for the screening effect in this kind of field. However, we understand this issue as indicating that the dielectric function can always be introduced into the formula at a phenomenological level.

In the scheme of our model, a key point is introducing an empirical PS to model the scattering of electrons, and the validity of the model resides in the empirical PS method (EPM). In the EPM, the total screened potential is approximated by a superposition of the full screened atomic PS which is the PS that we used [21]. And this decomposition process can always be operated in a local density approximation (LDA) sense [22]. This screened atomic PS can be used to reproduce the experimental data [18] and *ab initio* results for Si film [23] very well. Therefore, the behaviors of the scattering rate derived from our model are similar to those found from the conventional method including the screening effect (see the figure 2(a)). It is worth pointing out that the planar components of this field in our model induce roughness scattering directly, which is different to the case for the method developed where a vertical field is the source of scattering and manifests itself by modifying the energy levels, and so on [9].

The local fluctuation $\delta E(\mathbf{r})$ in the quantization energy caused by the fluctuation of the thickness of the film works as the scattering potential for the 2D electron motion in the conventional method [15, 24]. However, the scattering strength at each fluctuation site is wavevector independent; it can be dependent on q only after including the screening effect. In the present model, the PS generated by the SRSCs works as the scattering potential. The thickness dependence enters not only into a simple factor as $(\frac{\Omega_{\mathrm{atom}}}{2S_0L})^2$ but also into the PS. However it will be shown in the following that this model can fit the experimental data very well.

In figures 2(b) and (c), the SCR against q at different d and $\Delta_{\|}$ are shown. The position of the peak for $1/\tau_{1,\mathrm{AR}}$ moves to smaller q with larger d in figure 2(b). Because d characterizes the mean distance between the rough 'bumps' along the surface, larger d means less dramatic roughness and only longer waves can be effectively scattered between the 'bumps', while the peak of the SCR for $1/\tau^{S}_{1,\mathrm{BR}}$ is enhanced with larger d and its position moves to small q, slightly, which is somewhat different from the AR case. In figure 2(c), the magnitude of $1/\tau_{1,\mathrm{AR}}$ is greatly enhanced with increasing $\Delta_{\|}$, which characterizes the degree of roughness. Thus it can be understood as indicating that more transitions are induced by more SR. The variation of $1/\tau_{n,\mathrm{AR}}$ with the occupied subband index n is shown in figure 2(d). It can be observed that the SCR first increases with n until $n = 7$, and then it drops slightly to an asymptotic value at larger n. This indicates that SR becomes more dominant at higher charge density [2].

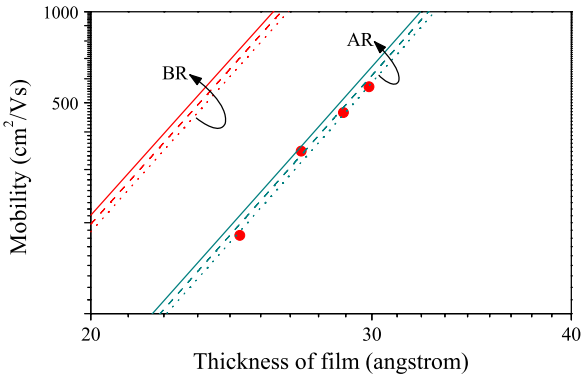

Figure 3. The thickness dependence of the mobility is shown. Solid, dashed and dotted lines for AR and BR cases correspond to $d = 1.5$ nm, $d = 1.6$ nm and $d = 1.7$ nm respectively. $\Delta_{\|} = 1a_0$, $n = 1$, $q = 5 \times 10^6$ cm^{-1}. Circular dots show the data from experiment [4].

In figure 3, the variation of the mobility with the thickness of the Si film is shown. We set the same d and same $\Delta_{\|}$ for the AR and BR cases to compare their contributions to the mobility at the same roughness level. It can be observed that the BR case gives weaker scattering, and the mobility in the AR case with $d = 1.7$ nm matches the values from experiment [4] very well (to compare with experiment, four-atomic-layer roughness is set, as estimated in experiments, which gives $\Delta_{\|} = a_0$), while the lines for the BR case cannot fit the experimental data well under the same parameters. Further investigations show (not indicated in figure) that there is no good parameter pair $(d, \Delta_{\|})$ for the BR case when $\Delta_{\|} = a_0$ is kept unaltered. However, one has the freedom to tune this parameter pair in a range. For example, ($d = 3.84$ nm, $\Delta_{\|} = 12.17$ Å) for the BR case gives a fair fit, but the value of $\Delta_{\|}$ is too large and not consistent with the experimental value, while the parameters for the AR case match experimental data and are therefore more reasonable. Additional detailed experimental data for the SR parameters are necessary to give an absolute comparison between these two models. Another characteristic is that the lines for the AR and BR cases are almost exactly parallel to each other, which indicates the same order thickness dependence of the mobility. The difference is that the same roughness configuration leads to stronger scattering in the AR case and weaker scattering in the BR case. Our model clearly gives a better result.

In summary, we have established a microscopic model for SR in the UTB MOSFET based on a diffraction pseudopotential method. The results from the present model are compared to those from the previously developed method and experiment. A very good consistency as regards mobility with experiment strongly supports the new model.

Acknowledgments

Z G Z thanks Dr Tony Low and Dr Chen Shen for various discussions. This work was supported under an A*STAR grant for Physical Modeling and Simulation of Nano-Scale Electronic Device Phenomena.

References

[1] Taur Y and Ning T H 2000 *Fundamentals of Modern VLSI Devices* (Cambridge: Cambridge University Press)
[2] Ando T *et al* 1982 *Rev. Mod. Phys.* **54** 437
[3] Ferry D K and Goodnick S M 1997 *Transport in Nanostructures* (Cambridge: Cambridge University Press)
[4] Uchida K *et al* 2002 *IEEE IEDM* p 47
[5] Thomas T R 1999 *Rough Surfaces* (London: Imperial College Press)
Bennett J M and Mattsson L 1989 *Introduction to Surface Roughness and Scattering* (Washington, DC: Optical Society of America)
[6] Prange R E and Nee T-W 1968 *Phys. Rev.* **168** 779
Saitoh M 1977 *J. Phys. Soc. Japan* **42** 201
[7] Matsumoto Y and Uemura Y 1974 *Japan. J. Appl. Phys. Suppl.* **2** 367 (Pt. 2)
[8] Ando T 1977 *J. Phys. Soc. Japan* **43** 1616
[9] Fischetti M V *et al* 2003 *J. Appl. Phys.* **94** 1079
Mou C-Yu and Hong T-M 2000 *Phys. Rev.* B **61** 12612
Jin S *et al* 2007 *IEEE Trans. Electron Devices* **54** 2191
[10] Low T *et al* 2004 *IEEE IEDM* p 151
Low T *et al* 2005 *IEEE Trans. Electron Devices* **52** 2430
[11] Evans M H *et al* 2005 *Phys. Rev. Lett.* **95** 106802
[12] Kittel C 1996 *Introduction to Solid State Physics* (New York: Wiley)
[13] Harrison W A 1966 *Pseudopotentials in The Theory of Metals* (New York: Benjamin)
[14] Chattopadhyay D and Queisser H J 1981 *Rev. Mod. Phys.* **53** 745
[15] Sakaki H *et al* 1987 *Appl. Phys. Lett.* **51** 1934
[16] Goodnick S M *et al* 1985 *Phys. Rev.* B **32** 8171
[17] Ishihara T *et al* 2002 *Japan. J. Appl. Phys.* I **41** 2353
Leadley D R *et al* 2002 *Semicond. Sci. Technol.* **17** 708
[18] Zhang S B *et al* 1993 *Phys. Rev.* B **48** 11204
[19] Stern F 1980 *Phys. Rev. Lett.* **44** 1469
[20] Stern F and Howard W E 1967 *Phys. Rev.* **163** 816
[21] Wang L-W and Zunger A 1994 *J. Phys. Chem.* **98** 2158
[22] Wang L-W and Zunger A 1995 *Phys. Rev.* B **51** 17398
[23] Zhu Z G *et al* 2008 *Semicond. Sci. Technol.* **23** 025009
[24] Ishihara T *et al* 2006 *Japan. J. Appl. Phys.* **45** 3125